Catalysis Today 138 (2008) 244–248

Contents lists available at ScienceDirect

Catalysis Today

journal homepage: www.elsevier.com/locate/cattod

Post-synthesis modifications of SBA-15 carbon replicas: Improving hydrogen storage by increasing microporous volume

M. Armandi [a,b], B. Bonelli [a,b,*], E.I. Karaindrou [a], C. Otero Areán [c], E. Garrone [a,b]

[a] Dipartimento di Scienza dei Materiali e Ingegneria Chimica, Politecnico di Torino, C.so Duca degli Abruzzi 24, I-10129 Torino, Italy
[b] INSTM Research Unit of Torino Politecnico, Italy
[c] Departamento de Química, Universidad de las Islas Baleares, 07122 Palma de Mallorca, Spain

ARTICLE INFO

Article history:
Available online 20 June 2008

Keywords:
Hydrogen storage
Microporous carbon
Microporous volume
NL-DFT
SBA-15 carbon replicas

ABSTRACT

SBA-15 carbon replicas were synthesized with a sucrose solution as carbon source, carrying out carbonization at two different temperatures (800 and 1000 °C). Carbon pyrolised at 800 °C showed higher BET surface area and was chosen for further post-synthesis activation treatments (physical via CO_2 or chemical via KOH), with the aim of improving hydrogen adsorption capacity. For comparison, an amorphous carbon was also synthesized, by direct carbonization of the carbon source, without any inorganic template: on this material a chemical activation was also performed. H_2 adsorption isotherms at the temperature of liquid nitrogen and sub-atmospheric pressure were measured. A linear correlation was found between hydrogen uptake and microporous volume of the different carbons, rather than with BET specific surface area. Surprisingly, the sample prepared in the absence of inorganic template resulted the most effective one.

1. Introduction

Storage of hydrogen, the ideal energy vector for replacing fossil fuels, is a challenge for material science [1]. The currently considered methods, *i.e.* liquid hydrogen; compressed gaseous hydrogen; hydrogen chemical storage in atomic form (as with metal hydrides) and hydrogen physisorption, present intrinsic limitations and technological problems, and yield results well below the ambitious goal of Department of Energy (DoE) of the United States, 6.5 wt.% at ambient temperature and pressure to be achieved by 2010 [2]. As far as physisorption is concerned, materials are envisaged interacting only weakly with molecular hydrogen [1], but characterized by a small specific weight and a huge specific surface area. Because of a lower specific weight, activated or nanostructured carbons and carbon nanotubes (CNTs) are systems of choice, for instance with respect to some other nanoporous materials, like zeolites [3], characterized by different pore architecture and chemical composition. With several porous solids, a linear correlation occurs between hydrogen uptake and specific surface area [4–15].

Heat of adsorption plays a crucial role: Bhatia and Myers [16] have shown that, for ambient temperature storage and delivery in the 30–1.5 bar pressure range, the optimum value for adsorption enthalpy change is about -5 kJ mol^{-1}. With carbons, an average enthalpy change of -5.8 kJ mol^{-1} is usually found and, consequently, an optimum operating temperature of 115 K may be predicted [16]. The same authors have also shown that, though changing pore shapes and adsorption temperatures, the highest enthalpy of adsorption of hydrogen is always found on carbons having a pore diameter in the range between 7.5 and 6.5 Å. For these reasons, carbons with high-surface area, but especially with a narrow micropore size distribution and an average pore diameter of ca. 7 Å should be eligible candidates for hydrogen physisorption.

Activated carbons, usually obtained by thermal treatment of low-cost materials, like coal or bitumen, suffer from several drawbacks, *e.g.* a wide and poorly controlled distribution of pore size and the presence of sulphur and metal impurities in the precursor.

Carbons characterized by a tailored porous structure could be therefore attractive not only in the field of gas storage media, but also for the development of advanced separation systems and in heterogeneous catalysis. The synthesis of ordered meso- and microporous carbons involves the use of mesoporous silica or

* Corresponding author at: Dipartimento di Scienza dei Materiali e Ingegneria Chimica, Politecnico di Torino, C.so Duca degli Abruzzi 24, I-10129 Torino, Italy. Tel.: +39 011 5644719; fax: +39 011 5644699.
E-mail address: barbara.bonelli@polito.it (B. Bonelli).

0920-5861/$ – see front matter © 2008 Elsevier B.V. All rights reserved.
doi:10.1016/j.cattod.2008.05.002

zeolites as a template [17–25]. The procedure consists in the infiltration of the inorganic template with an appropriate carbon source, followed by carbonization of the precursor and subsequent removal of the inorganic template with an HF solution.

Depending on the type of inorganic template, carbons with different structures and pore sizes may be prepared: this work reports on the synthesis and modification of carbon replicas of SBA-15 mesoporous silica. The effect of both pyrolysis temperature and post-synthesis treatments have been investigated. Two classical methods were applied as post-synthesis modifications, *i.e.* a treatment in CO_2 flow (physical activation) and a treatment with KOH (chemical activation). In order to elucidate the role of microporosity, a disordered microporous carbon has also been prepared, by carbonization of the same carbon precursor (an acidic aqueous solution of sucrose) in the absence of inorganic template, and by activating the obtained product with KOH.

Hydrogen adsorption on these materials was studied at the temperature of liquid nitrogen and sub-atmospheric pressures, since previously reported results [26,27] were collected on similar materials in the same conditions.

2. Experimental

2.1. Materials

SBA-15 silica was prepared, following Zhao et al. [28], by using a non-ionic oligomeric alkyl-ethylene oxide surfactant (Pluronic 123) as structure directing agent. After template removal by calcination at 500 °C in flowing air, this mesoporous silica was impregnated with an acidic solution of sucrose, according to Ref. [18]. Carbonization was performed by heating in a tubular furnace under N_2 flow at 800 and at 1000 °C (heating rate 2 °C min^{-1}), obtaining the samples termed C-800 and C-1000, respectively. Finally, silica was removed by leaching with an aqueous solution of HF (5 wt.%).

With C-800 sample, which showed better textural properties than C-1000, further post-synthesis activations were performed: (i) physical activation (sample C-Phys) and (ii) chemical activation (sample C-Chem):

(i) 1 g of C-800 was heated at 800 °C under N_2 flow, then gas flow was switched to CO_2. After 1 h, the sample was cooled to r.t. under nitrogen flow. In the literature [29], this type of treatment is generally indicated as "physical activation", even if it probably involves a gasification reaction between carbon and carbon dioxide.
(ii) 1 g of C-800 was mixed with water and KOH (carbon/KOH weight ratio 1/1). After drying, the mixture was treated at 800 °C for 1 h, under nitrogen flow. Finally, it was washed with 0.1 M HCl and hot bi-distilled water, in order to remove excess KOH, and dried.

A disordered porous carbon (sample CS128) was prepared by carbonization of the acidic solution of sucrose, used to produce C-800 and C-1000 carbons, at 150 °C; the product was then mixed with a KOH aqueous solution (carbon/KOH weight ratio 1/2) and dried overnight at 100 °C; the resulting mixture was treated at 800 °C under nitrogen flow, washed with 0.1 M HCl and hot bi-distilled water and dried.

2.2. Characterization methods

X-rays diffraction (XRD) patterns were collected on a X'Pert Phillips diffractomer using Cu Kα radiation, in the following conditions: range = (0.8–4)2θ; step width 2θ = 0.02; time per step = 10 s. Brunauer–Emmet–Teller (BET) surface area measurement and pore size analysis were carried out on powders previously outgassed at 250 °C, by N_2 sorption at 77 K on a Quantachrome Autosorbe 1C instrument. Microporous volumes were calculated according to the *t*-plot method; the Barrett–Joyner–Halenda (BJH) method was used to determine average mesopore diameter.

Field-emission scanning electron microscopy (FESEM) pictures were collected on a high-resolution FE-SEM instrument (LEO 1525) equipped with a Gemini field emission column; with the same instrument, the possible occurrence of residual potassium was checked by energy dispersive X-rays (EDX) analysis.

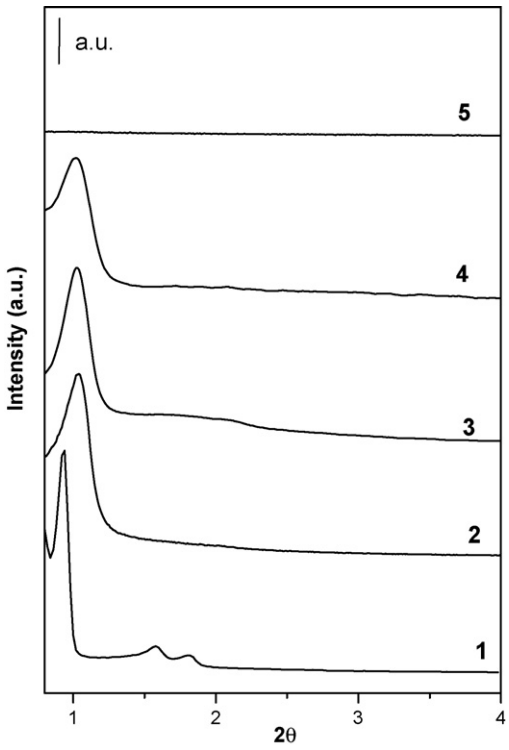

Fig. 1. Low-angle XRD patterns of parent SBA-15 (curve 1) and of C-800, C-1000, C-Phys and C-Chem carbon replicas (curves 2, 3, 4 and 5, respectively).

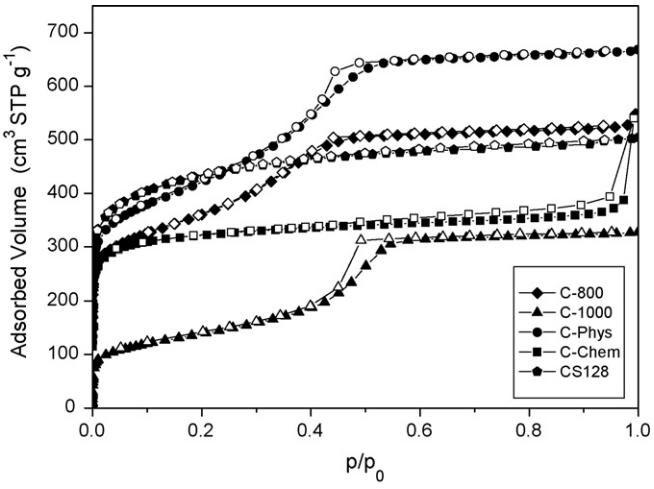

Fig. 2. N_2 adsorption/desorption isotherms at −196 °C on C-800 (diamonds), C-1000 (triangles), C-Phys (circles), C-Chem (squares) and CS128 (pentagons).

Table 1
Textural properties of parent SBA-15 silica and of carbon materials, as determined by combined XRD and N_2 adsorption at −196 °C

Material	S_{BET} ($m^2\ g^{-1}$)	BJH[a], mesopores diameter (Å)	NL-DFT[b], mesopores diameter (Å)	V_{tot} ($cm^3\ g^{-1}$)	*t*-Plot V_{micro} ($cm^3\ g^{-1}$)	Lattice parameter *a* (Å)[c]
SBA-15	770	70	–	0.80	0.06	108
C-800	1000	30	29–33	0.75	0.09	98
C-1000	520	38	38	0.50	0.04	99
C-Phys	1440	36	36	1.00	0.22	98
C-Chem	1200	–	–	0.58	0.44	–
CS128	1520	–	–	0.78	0.60	–

[a] As evaluated from the adsorption branch, the BJH algorithm having been followed.
[b] As determined by the NL-DFT method.
[c] Lattice parameters were calculated according to the formula $2(3^{-1/2})d_{1\,0\,0}$.

Hydrogen adsorption isotherms at the temperature of liquid nitrogen (−196 °C) and sub-atmospheric pressure were measured on powders (about 50 mg) previously outgassed at 250 °C (Quantachrome Autosorb 1C), the estimated accuracy of measured volumes being ±1 $cm^3\ g^{-1}$. Each isotherm was performed twice, in order to check reproducibility.

3. Results and discussion

3.1. Textural properties

Fig. 1 reports low-angle XRD patterns of parent SBA-15 silica (curve 1) and samples C-800, C-1000, C-Phys and C-Chem (curves 2–5). Low-angle XRD patterns of CS128 are not reported, since no structural order is expected for this sample.

For SBA-15, three well-resolved peaks are observed, corresponding to (1 0 0), (1 1 0) and (2 0 0) reflections typical of the 2D hexagonal space group *p6mm*. The corresponding cell parameter, *a*, as calculated from the (1 0 0) reflection according to the relation $a = 2(3^{-1/2})d_{1\,0\,0}$, was 108 Å.

For C-800 and C-1000 samples, the main diffraction peak is maintained, indicating that rather ordered mesoporous materials with hexagonal structures were obtained. The expected loss of long-range order, as observed by the disappearing of reflections at higher 2θ values, is limited. With respect to parent silica, a shift of $d_{1\,0\,0}$ peak towards higher 2θ values is observed, in agreement with the literature [17,18]: the observed decrease of the corresponding lattice parameter to 98–100 Å (Table 1) is probably due to shrinkage of the silica template framework during carbonization [30].

For C-Phys, the $d_{1\,0\,0}$ peak is also maintained, indicating that the hexagonal structural order is preserved, whereas in C-Chem the structural order was completely lost.

Fig. 2 reports N_2 adsorption–desorption isotherms at −196 °C. By subtracting BJH pore size from cell parameter values (Table 1), the silica wall thickness was calculated to be about 38 Å, in agreement with literature data [31]: this value is close to the mesopore diameter of the obtained carbons, showing that replicas of the silica template were actually attained.

The C-800 sample has a high-BET surface area (1000 $m^2\ g^{-1}$), a BJH pore diameter of 30 Å and a microporous volume of 0.09 $cm^3\ g^{-1}$. Upon increasing carbonization temperature, an increase in mesopores diameter is observed, probably due to a higher volume contraction of carbon precursor at higher tem-

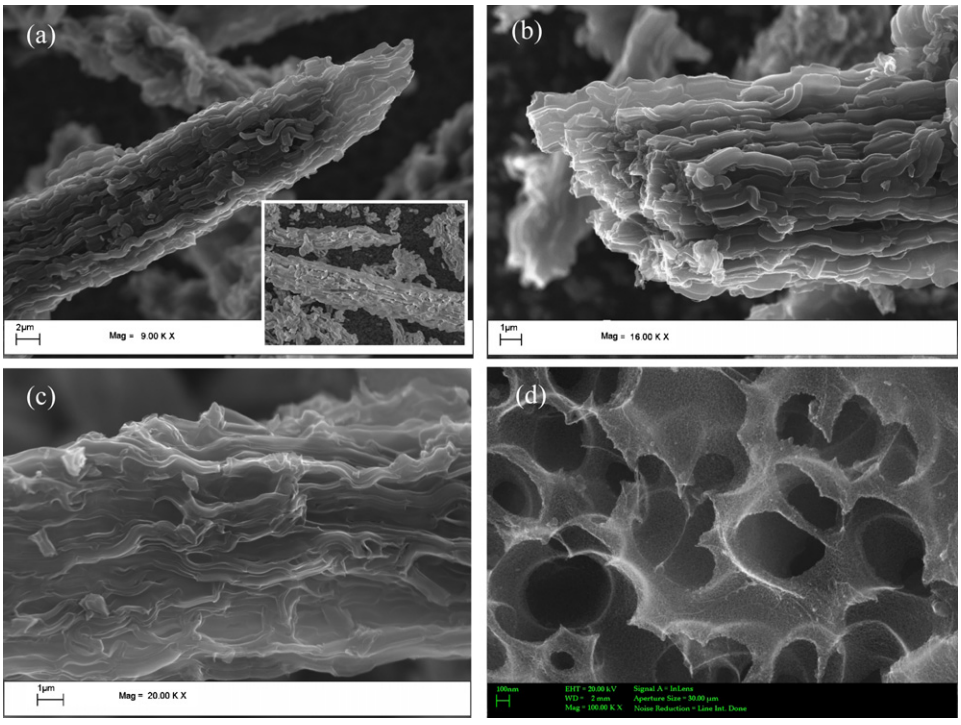

Fig. 3. FESEM pictures of C-800 (a), C-Phys (b), C-Chem (c), CS128 (d) and parent SBA-15 (inset to (a)).

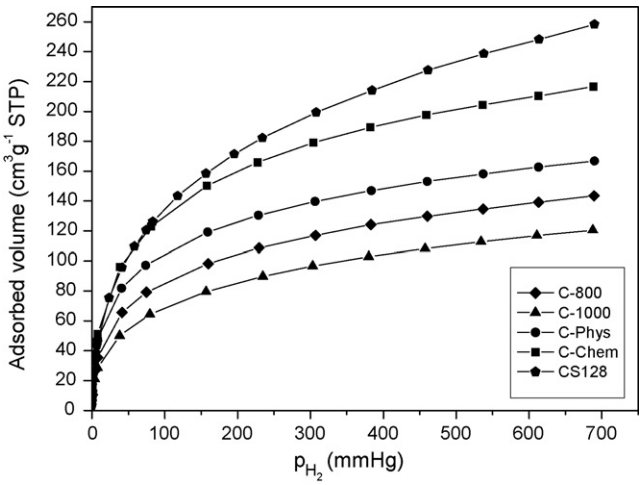

Fig. 4. Hydrogen adsorption isotherms at −196 °C on C-800 (diamonds), C-1000 (triangles), C-Phys (circles), C-Chem (squares) and CS128 (pentagons).

peratures. For C-1000, a decrease of BET surface area (520 $m^2\ g^{-1}$) and microporous volume (0.04 $cm^3\ g^{-1}$) is observed. A higher volume contraction of the carbon precursor along with an increased degree of graphitization at 1000 °C probably contribute to such changes in textural properties [32–34].

The C-Phys sample still exhibits a Type IV isotherm, with a more pronounced hysteresis loop with respect to parent C-800. The heat-treatment with CO_2 caused an increase in BET surface area to 1440 $m^2\ g^{-1}$, in total pore volume and in micropore volume (now 1.0 and 0.22 $cm^3\ g^{-1}$, respectively). For C-Chem, a Type I isotherm is observed, typical of microporous systems: the total pore volume is basically due to micropores (0.44 $cm^3\ g^{-1}$ against 0.58 $cm^3\ g^{-1}$). As to mesopores, activation with CO_2 leads to an increase in average mesopore diameter (36 Å), while treatment with KOH brings about (i) the disappearance of mesopores and (ii) an increase of BET surface area and microporous volume. Most probably, these two effects are due, respectively, to (i) KOH leaching of carbon spacers connecting carbon nanorods, with consequent collapse of the ordered structure, and (ii) to chemical attack of nanorods by KOH in such a way that microchannels are formed perpendicularly to nanorods, leading to increased microporosity.

CS128 has the highest BET surface area (1520 $m^2\ g^{-1}$), exhibiting, as C-Chem, a Type I isotherm: its total pore volume is mainly due to micropores (0.60 $cm^3\ g^{-1}$ against 0.78 $cm^3\ g^{-1}$). This result indicates that KOH attack is probably the main responsible for micropores formation. It must be pointed out that EDX analysis measured a residual potassium amount of about 2.7% by weight, in contrast with C-Chem sample where no potassium was found.

Fig. 3 reports FESEM pictures of prepared materials. The rope-like morphology of parent SBA-15 (inset to Fig. 3a) is observed for all carbon replicas (Fig. 3a–c), but C-Chem (Fig. 3c), carbon particles appear to be rather "frayed" by KOH leaching. Interestingly, CS128 shows a sponge-like structure of particles having irregular morphology (Fig. 3d).

3.2. Hydrogen adsorption isotherms at the temperature of liquid nitrogen

Fig. 4 reports hydrogen adsorption isotherms at −196 °C, in the 1–700 mmHg pressure range. With all carbons, hydrogen adsorption resulted to be completely reversible, with no hysteresis phenomena. In the adopted experimental conditions, the following order in H_2 uptake was observed: CS128 > C-Chem > C-Phys > C-800 > C-1000. The highest uptake was shown by CS128, with an adsorbed hydrogen volume of 258 $cm^3\ g^{-1}$, corresponding to an overall uptake of 2.4% by weight.

Adsorbed volumes of hydrogen at 700 mmHg and −196 °C are plotted as a function of samples BET surface areas (Fig. 5a) and microporous volumes (Fig. 5b). In the former case, the regular trend reported repeatedly in the literature for different porous systems [1,35–38] is not observed. In the latter case, instead, a linear correlation is observed for all samples, which definitely points out to the crucial role of microporosity in H_2 adsorption, as previously proposed for several ordered porous carbons [27,39,40], activated carbons and activated carbon fibres [41]. Question may arise whether residual potassium may affect H_2 physisorption on CS128, especially by considering previous works on high-H_2 uptake by alkali-doped CNTs obtained by solid-state reactions with salts [6,42]: it must be pointed out that in the latter case, potassium was shown to favour the dissociation of hydrogen, which further reacts with CNTs, giving rise to a partially irreversible chemical storage of hydrogen in different experimental conditions (*i.e.* higher temperature) [6]. In the present case, H_2 adsorption was completely reversible, as checked by performing two adsorption/desorption cycles. Should potassium favour H_2 physisorption, one would expect a higher H_2 uptake than that obtained on account of the increased micropore volume.

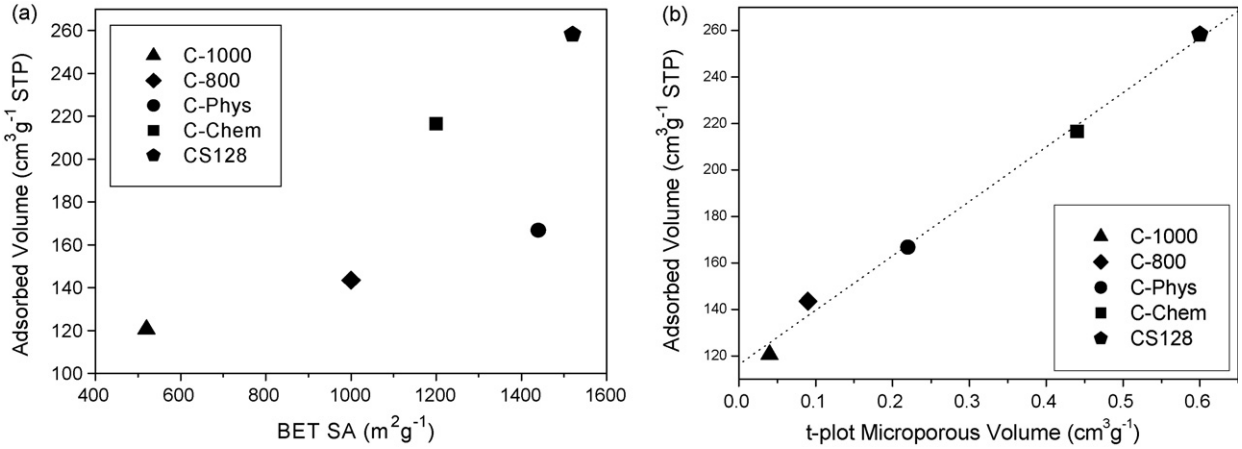

Fig. 5. Volumes of adsorbed H_2 (at −196 °C and 700 mmHg) reported as a function of samples BET specific surface areas (a); correlation among adsorbed volumes of H_2 and microporous volumes of carbons, as evaluated by the *t*-plot method (b).

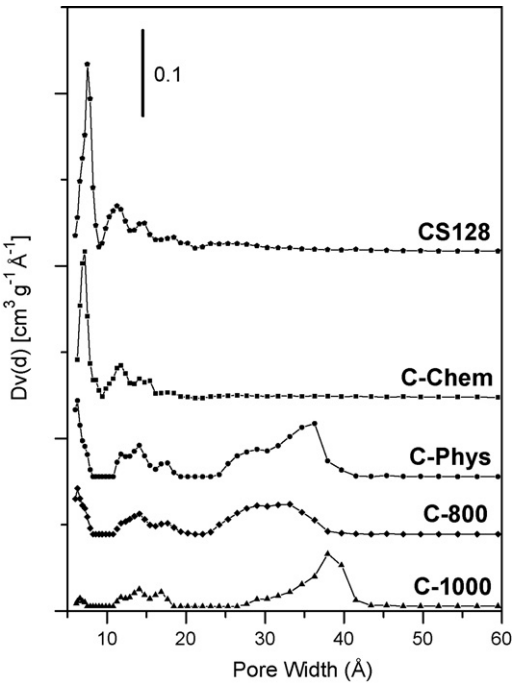

Fig. 6. Pore size distribution (PSD), as calculated by the NL-DFT method, for C-800 (diamonds), C-1000 (triangles), C-Phys (circles), C-Chem (squares) and CS128 (pentagons).

For a detailed study of porosity of the obtained carbons, volumetric data obtained from N_2 adsorption isotherms at −196 °C were analyzed by using the NL-DFT method, by applying the kernel for N_2 adsorption at −196 °C on carbon having slit shaped pores. Corresponding pore size distributions (PSD) are reported in Fig. 6 the obtained mesopore size values are in good agreement with those calculated by the BJH method (see Table 1 for comparison). Fig. 6 clearly shows that the main effect of carbonization temperature on PSD is the disappearance of narrow micropores in the C-1000 sample. As to the influence of post-synthesis treatment on PSD, two effects may be pointed out: (i) the disappearance of mesoporosity for sample C-Chem and (ii) a progressive increase in the population of 7 Å micropores when passing from C-800, to C-Phys and C-Chem. Such narrow micropores are even more abundant in CS128, the sample giving the best results in terms of hydrogen uptake, and could therefore be the main actors in the hydrogen adsorption process.

4. Conclusions

The results reported in the present paper show that the classical post-synthesis treatment of carbons with either carbon dioxide (“physical”) or KOH (“chemical”) have a deep effect also on SBA-15 carbon replicas. The structural order is preserved after physical activation, but not after chemical treatment. With respect to the pristine carbon replica, higher BET surface areas and microporous volumes were measured in both cases; in particular, chemical activation resulted to be very effective in the formation of highly microporous carbon. However, a disordered carbon sample, prepared without template and further activated with KOH, showed both the highest BET surface area and the highest microporous volume.

For the SBA-15 carbon replicas, hydrogen uptake at −196 °C was found to be in the order: C-Chem > C-Phys > C-800 > C-1000. However, the highest hydrogen uptake was shown by a microporous carbon sample (CS128) obtained without template; this sample was found to adsorb a volume of 258 cm^3 of hydrogen per gram of carbon, which corresponds to ∼2.4 wt.%.

A linear correlation between hydrogen adsorption capacity and micropore volume was found for all samples, so confirming that micropores play a crucial role in hydrogen adsorption on this type of materials, in particular as far as narrow micropores with 7 Å diameter are concerned.

Acknowledgements

The authors wish to acknowledge Regione Piemonte (CIPE Project C72) and MUR (Ministero dell'Università e della Ricerca—FISR Project Vettore Idrogeno) for financial support.

References

[1] A. Züttel, Mater. Today 6 (2003) 24–33, and references therein.
[2] S. Hynek, W. Fuller, J. Bentley, Int. J. Hydrogen Energy 22 (6) (1997) 601.
[3] J. Weitkamp, M. Fritz, S. Ernst, Int. J. Hydrogen Energy 20 (12) (1995) 967.
[4] A. Chambers, C. Park, R.T.K. Baker, N.M. Rodriguez, J. Phys. Chem. B 102 (22) (1998) 4253.
[5] A.C. Dillon, K.M. Jones, T.A. Bekkedahl, C.H. Kiang, D.S. Bethune, M.J. Heben, Nature 386 (1997) 377.
[6] P. Chen, X. Wu, J. Lin, K.L. Tan, Science 285 (1999) 91.
[7] C. Carpetis, W. Peschka, Int. J. Hydrogen Energy 5 (1980) 539.
[8] J.S. Noh, R.K. Agarwal, J.A. Schwarz, Int. J. Hydrogen Energy 12 (1987) 693.
[9] K.A.G. Amankwah, J.S. Noh, J.A. Schwarz, Int. J. Hydrogen Energy 14 (1989) 437.
[10] R. Chaine, T.K. Bose, Int. J. Hydrogen Energy 19 (1994) 161.
[11] M. Conte, P.P. Prosini, S. Passerini, Mater. Sci. Eng. B 108 (2004) 2.
[12] M. Hirscher, M. Becher, M. Haluska, F von Zeppelin, X. Chen, U. Dettlaff-Weglikowska, S. Roth, J. Alloys Compd. 356–357 (2003) 433.
[13] H.M. Cheng, Q.H. Yang, C. Liu, Carbon 39 (10) (2001) 1447.
[14] F. Lamari-Darkrim, P. Malbrunot, G.P. Tartaglia, Int. J. Hydrogen Energy 27 (2) (2002) 193.
[15] A. Züttel, P. Sudan, Ph. Mauron, T. Kiyobayashi, Ch. Emmenegger, L. Schlapbach, Int. J. Hydrogen Energy 27 (2) (2002) 203.
[16] S.K. Bhatia, A.L. Myers, Langmuir 22 (4) (2006) 1688.
[17] J.S. Lee, S.H. Joo, R. Ryoo, J. Am. Chem. Soc. 124 (7) (2002) 1156.
[18] S. Jun, S.H. Joo, R. Ryoo, M. Kruk, M. Jaroniec, Z. Liu, T. Ohsuna, O. Terasaki, J. Am. Chem. Soc. 122 (43) (2000) 10712.
[19] T. Kyotani, T. Nagai, S. Inoue, A. Tomita, Chem. Mater. 9 (2) (1997) 609.
[20] P.M. Barata-Rodrigues, T.J. Mays, G.D. Moggridge, Carbon 41 (12) (2003) 2231.
[21] H. Darmstadt, C. Roy, S. Kaliaguine, S.J. Choi, R. Ryoo, Carbon 40 (14) (2002) 2673.
[22] S.H. Joo, S. Jun, R. Ryoo, Micropor. Mesopor. Mater. 44–45 (2001) 153.
[23] J. Kim, J. Lee, T. Hyeon, Carbon 42 (12–13) (2004) 2711.
[24] A.B. Fuertes, S. Alvarez, Carbon 42 (15) (2004) 3049.
[25] A.B. Fuertes, D.M. Nevskaia, Micropor. Mesopor. Mater. 62 (3) (2003) 177.
[26] J. Pang, J.E. Hampsey, Z. Wu, Q. Hu, Y. Lu, Appl. Phys. Lett. 85 (21) (2004) 4887.
[27] R. Gadiou, S.E. Saadallah, T. Piquero, P. David, J. Parmentier, C. Vix-Guterl, Micropor. Mesopor. Mater. 79 (1–3) (2005) 121.
[28] D. Zhao, J. Feng, Q. Huo, N. Melosh, G.H. Fredrickson, B.F. Chmelka, G. Stucky, Science 279 (1998) 548.
[29] A. Ahmadpour, D.D. Do, Carbon 34 (1995) 471, and references therein.
[30] H.J. Shin, R. Ryoo, M. Kruk, M. Jaroniec, Chem. Commun. (2001) 349.
[31] D. Zhao, Q. Huo, J. Feng, B.F. Chmelka, G. Stucky, J. Am. Chem. Soc. 120 (1998) 6024.
[32] D.J. Kim, H.I. Lee, J.E. Yie, S.J. Kim, J.M. Kim, Carbon 43 (2005) 1868.
[33] M. Sevilla, A.B. Fuertes, Carbon 44 (2006) 468.
[34] M. Armandi, B. Bonelli, I. Bottero, C. Otero Areán, E. Garrone, Micropor. Mesopor. Mater. 103 (2007) 150.
[35] A. Zecchina, S. Bordiga, J.G. Vitillo, G. Ricchiardi, C. Lamberti, G. Spoto, M. Bjørgen, K.P. Lillerud, J. Am. Chem. Soc. 127 (2005) 6361.
[36] J.L.C. Rowsell, A.R. Millward, K.S. Park, O.M. Yaghi, J. Am. Chem. Soc. 126 (2004) 5666.
[37] S.S. Kaye, J.R. Long, J. Am. Chem. Soc. 127 (2005) 6506.
[38] M.G. Nijkamp, J.E.M.J. Raaymakers, A.J. van Dillen, K.P. de Jong, Appl. Phys. A 72 (2001) 619.
[39] B. Fang, H. Zhou, I. Honma, J. Phys. Chem. B 110 (2006) 4875.
[40] C. Vix-Guterl, E. Frakowiak, K. Jurewicz, M. Friebe, J. Parmentier, F. Beguin, Carbon 43 (2005) 1293.
[41] M.A. de la Casa-Lillo, F. Lamari-Darkrim, D. Cazorla-Amoros, A. Linares-Solano, J. Phys. Chem. B 106 (2002) 10930.
[42] G.E. Froudakis, Nano Lett. 1 (2001) 531.